



Modeling the drying shrinkage of structural concretes

Abderraouf Kebir¹ · Abdelmalek Brahma¹

Received: 2 September 2020 / Accepted: 12 April 2021 / Published online: 28 May 2021
© Springer Nature Switzerland AG 2021

Abstract

Shrinkage in hydraulic materials is a complex time-dependent process. For standard concretes, one of the most considerable parts of shrinkage is drying shrinkage. In fact, to predict deformations of concrete due to shrinkage, various predictive models have been developed; most of them use many numbers of factors that can affect shrinkage such as concrete strength, concrete age of loading, curing conditions type, ambient conditions, type of cement and aggregates, water to cement ratio, concrete mix, member shape and size, loading duration and type. Such a number of parameters increases the complexity of using these models and leads to some prediction imperfections; thence a new simplified model is needed. The main target of the current paper is to formulate a novel and simplified model with a minimum of factors that affect drying shrinkage behavior as relative humidity and volume to surface area ratio of the concrete element (V/S). To achieve this goal, a prediction model based on probability density function and a small number of parameters that influence shrinkage, as well as relative humidity and volume to surface area ratio of the concrete element, has been developed. A huge database has been used to adjust the model's parameters using the most recent studies and research to validate the model. The comparison of the model predictions with experimental results reveals that the simplified model is well adapted to represent and describe the evolution of drying shrinkage for normal, high-performance, lightweight, and self-compaction concretes, whereas there is negligible prediction divergence as compared to other existed models.

Keywords Hydraulic materials · Drying shrinkage · Modeling · Prediction

Introduction

To predict concrete shrinkage behavior, diverse analytical models have been elaborated and some of them are approved by diverse codes and recommended by famous researchers [1].

Shrinkage is affected by multiple variables as well as concrete strength, concrete loading time, cement type, type of curing conditions, ambient conditions, water to cement ratio, concrete mix, member size and shape, aggregates type, duration, and type of loading [2]. This large number of parameters affecting shrinkage increases the complexity of utilizing these models and can lead to imperfections in shrinkage predictions. It can also reduce databases exploitable results due to the lack of one or more of these parameters. Thence, a new simplified prediction model containing fewer parameters that affect shrinkage phenomena is necessary. The

quality of the shrinkage predictive model depends on the contribution of each parameter that conducts the phenomena [3]. In its report 209.1R-2 [1], the American Concrete Institute (ACI) defines shrinking as the deformation measured on a load-free concrete sample. ACI states that shrinkage excludes changes in length due to temperature variations, but it depends on the environment, configuration, and size of the specimen.

Researchers must often describe and analyze phenomena in diverse areas of science, with actions understood only from laboratory observations. For this reason, the synthesis of a mathematical model with similar behavior to the actual phenomenon is of interest. In particular cases, with the understanding of the model parameters and the experience requirement of the phenomenon, researchers can suggest a mathematical model named a deterministic model. The exact mechanisms of the phenomenon, though, are generally unknown. They might, therefore, formulate a mathematical model on which they determine the parameters of measurements from samples.

✉ Abderraouf Kebir
kebirgc@gmail.com

¹ Saad Dahleb University, Blida, Algeria

The drying shrinkage in concretes is the most significant part of shrinkage deformations [4]; it results from the reduction in pores relative humidity which increases directly the capillary tension of pores occupied by water and in the solid surface tension at pore walls. The data from experimental results shows that the measured ultimate values of concrete drying shrinkage of many specimens had a nonlinear function of ambient relative humidity [5].

This study aims to develop a representative prediction model of drying shrinkage for hydraulic materials with fewer affecting factors and more predictive accuracy. This manuscript is structured in the following way: First, the relation between drying shrinkage development and the probability density function was exposed. A step-by-step presentation of the demonstration that leads from mathematical density function to a model that can describe the drying shrinkage evolution was reviewed, these model parameters were been estimated by using large experimental results gathered from different databases. The obtained model was simplified to reduce its number of parameters. Once the model is established, we proceed to its validation and confront it with different types of concrete such as normal concrete (NC), high-performance concrete (HPC), lightweight concrete (LWC), and self-compacting concrete (SCC) as well as with most common models and various databases. Finally, the last section summarizes the main conclusions.

Experimental investigation

The present research is based on a vast range of experimental results obtained in various American and European laboratories by internationally renowned researchers [6, 7].

The experimental results analyzed are those that include the most parameters influencing the drying shrinkage.

Analytical investigation

Over the past few decades, researchers have proposed about 10 shrinkage prediction models based on a big database of experimental results.

Shrinkage in concrete structures is the most doubtful characteristic of concrete, taking into account material varieties and modeling unpredictability. Previous research is based on inputting determinate values of factors influencing shrinkage in order to obtain a structural response. However, researches on the shrinkage effects on concrete systems have become particularly important in recent years. The key factors of uncertainty are the alteration of climate conditions, the disparity in the composition and mixing of the concrete, and the variance due to the intrinsic shrinking process. It is well known that both of these models are mathematical or semi-theoretical

formulas, and the parameters of these models are derived through test-data fitting.

In this section, the most common models utilized for predicting the shrinkage deformation are quickly presented such as the B3 model, established by Bažant and Baweja [4, 5], the ACI 209R-92 model, established by Christianson and Branson [8], the GL 2000 model, established by Lockman and Gardner [9], the CEB MC 90 model [6] in addition to the modified CEB MC90-99 model [7], each of them established by Müller and Hilsdorf, and finally, the *fib* model [10], highlighting the approach to understand how the shape and size of the concrete element and the curing conditions, as well as the relative humidity, influence the predicted shrinkage deformations.

Whereas a factor dependent on the shape and size of the concrete element is used in the EC2 and also *fib* shrinkage models for determining exactly how shape and size influence the prediction deformations, the member volume to surface ratio is also used by ACI prediction model [3].

Euro code 2 shrinkage prediction model

The ultimate drying shrinkage deformation is defined by the Euro code 2 shrinkage model as in Eq. (1).

$$\varepsilon_{cd,\infty} = k_h \cdot \varepsilon_{cd,0} \quad (1)$$

where the basic drying shrinkage deformation is $\varepsilon_{cd,0}$ and k_h is a factor function of shape and size of the concrete element (in millimeters).

$$h_0 = 2 \cdot A_c / U \quad (2)$$

In Eq. (2), A_c represents the cross-section area and U is the concrete element circumference subject to drying. The basic drying shrinkage deformation as is mentioned in Eq. (3) is a compressive strength function f_{cm} , where $f_{cm0} = 10$ MPa, both factors α_{ds1} and α_{ds2} define the cement type, and the ambient relative humidity RH.

$$\varepsilon_{cd,0} = 0.85 \cdot \left[(220 + 110 \cdot \alpha_{ds1}) \cdot \exp\left(-\alpha_{ds2} \cdot \frac{f_{cm}}{f_{cm0}}\right) \right] \cdot 10^{-6} \cdot \beta_{RH} \quad (3)$$

Relative humidity RH is expressed by the β_{RH} coefficient Eq. (4).

$$\beta_{RH} = 1.55 \cdot \left[1 - \left(\frac{RH}{RH_0} \right)^3 \right] \quad (4)$$

with $RH_0 = 100\%$.

The drying shrinkage deformation progression is a time function as is mentioned in Eq. (5).

$$\varepsilon_{cd}(t) = \varepsilon_{cd,0} \cdot k_h \cdot \beta_{ds}(t, t_s) \quad (5)$$

With;

$$\beta_{ds}(t, t_s) = \frac{(t - t_s)}{0.04\sqrt{h_0^3 + (t - t_s)}} \tag{6}$$

Also, t , t_s (in days) are the present age and the beginning drying concrete age, respectively. Therefore, in the Euro code 2 shrinkage model, the h_0 value is employed a couple of times, for example in k_h factor, affecting the ultimate drying shrinkage deformation, and in $\beta_{ds}(t, t_s)$ Eq. (6), affecting the shrinkage deformation progress.

ACI 209R-92 shrinkage model

The ultimate shrinkage deformation for conventional conditions is defined by the ACI 209R-92 Eq. (7).

$$\epsilon_{shu} = 780 \times 10^{-6} \cdot \gamma_{sh} \tag{7}$$

where γ_{sh} is a corrective coefficient represented by seven corrective terms are: the curing method ($\gamma_{sh,tc}$), the ambient relative humidity ($\gamma_{sh,RH}$), the volume to surface area ratio ($\gamma_{sh,vs}$) or, otherwise, the concrete element thickness ($\gamma_{sh,d}$), the concrete slump ($\gamma_{sh,s}$), the fine aggregate proportion ($\gamma_{sh,\psi}$), the cement content ($\gamma_{sh,c}$) and the concrete air content ($\gamma_{sh,\alpha}$).

The shrinkage strain evolution is similar to the Euro code 2 shrinkage model Eq. (8).

$$\epsilon_{sh}(t, t_c) = \frac{(t - t_c)^\alpha}{f + (t - t_c)} \cdot \epsilon_{shu} \tag{8}$$

where α is defined by a time-related function ($\alpha = 1$), t and t_s (in days) are the present age and the beginning drying concrete age, respectively, and f is a function Eq. (9).

$$f = 26 \cdot e^{\{10 \times 1.42 - 2 \cdot (V/S)\}} \tag{9}$$

With, V/S is the member volume to surface ratio (in millimeters) to take into account the size and shape influence on concrete shrinkage.

Similar to the Eurocode2 shrinkage model, the ACI 209R-92 model considers the size and shape impact a couple of times, for example in the correcting coefficient $\gamma_{sh,vs}$ or $\gamma_{sh,d}$, affecting γ_{sh} , and therefore the ultimate shrinkage deformation ϵ_{shu} Eq. (7), and in the volume to surface ratio V/S in the function f Eq. (9), affecting the shrinkage deformation progress.

As reported in ACI 209R-92 model, the impact of concrete elements size on the ultimate shrinkage deformation can even be taken into account by the correction coefficient $\gamma_{sh,vs}$, or by the correction coefficient $\gamma_{sh,d}$ for concrete elements with average thickness other than 150 mm as reported in Eq. (10).

$$d = 4 \cdot V/S \tag{10}$$

Furthermore to values given for $\gamma_{sh,d}$ for $d < 150$ mm, equations for calculating $\gamma_{sh,d}$ for $150 \text{ mm} < d < 380$ mm are also delivered. Therefore, contrary to the EC2 shrinkage model, the ACI 209R-92 model is planned to be useful only to concrete elements of restricted average thickness.

B3 shrinkage model

The predicted ultimate shrinkage strain of Bažant-Baweja B3 shrinkage model is given as in Eq. (11).

$$\epsilon_{sh\infty} = -\epsilon_{s\infty} \frac{E_{cm607}}{E_{cm(t_c + \tau_{sh})}} \tag{11}$$

The $\epsilon_{s\infty}$ factor relies on several parameters as well as the water content w , the concrete mean compressive strength at 28 days f_{cm28} , and constants α_1 and α_2 , the first one to take into account the cement type and the second for the curing condition as is mentioned in Eq. (12).

$$\epsilon_{s\infty} = -\alpha_1 \alpha_2 [0.019w^{2.1} f_{cm28}^{-0.28} + 270] \times 10^{-6} \tag{12}$$

The $\frac{E_{cm607}}{E_{cm(t_c + \tau_{sh})}}$ ratio is given as in Eq. (13)

$$\frac{E_{cm607}}{E_{cm(\tau_{sh} + t_c)}} = \left[\frac{1.0805}{[\tau_{sh} + t_c]^{0.5}} \right] + \left[\frac{1.0805}{[(0.85(\tau_{sh} + t_c) + 4)]^{-0.5}} \right] \tag{13}$$

where t_c defines the concrete age at the drying beginning and τ_{sh} represents the size relying on the shrinkage as is mentioned in Eq. (14).

$$\tau_{sh} = 0.085 t_c^{-0.08} f_{cm28}^{-0.25} [2k_s(V/S)]^2 \tag{14}$$

The cross-section correction shape coefficient is defined with k_s ($k_s = 1$ for easier calculations) and V/S is the volume to surface area ratio.

The development of the shrinkage deformation ϵ_{sh} Eq. (15) in EC2 and ACI 209R-92 shrinkage models is determined by multiplication of the ultimate shrinkage strain $\epsilon_{sh\infty}$ by a time function Eq. (16) and by humidity

$$\epsilon_{sh}(t, t_c) = -\epsilon_{sh\infty} k_h S(t - t_c) \tag{15}$$

$$S(t - t_c) = \tanh \sqrt{\frac{(t - t_c)}{\tau_{sh}}} \tag{16}$$

dependence coefficient k_h (e.g., $k_h = 1 - h^3$ for $h \leq 0.98$, with h is the relative humidity defined as a decimal). The size effect on shrinkage is expressed in Eq. (15) by the volume to surface ratio V/S for both the ultimate shrinkage deformation and the shrinkage progress.

GL2000 shrinkage model

The ultimate shrinkage deformation ϵ_{shu} is defined by the GL 2000 shrinkage prediction model as a function of the mean compressive strength of concrete at 28 days f_{cm28} and the shrinkage constant k as is mentioned in Eq. (17) with k is the cement type effect factor.

$$\epsilon_{shu} = 900k \left(\frac{30}{f_{cm28}} \right)^{1/2} \times 10^{-6} \tag{17}$$

Both the B3 and GL 2000 shrinkage models express the time-dependent shrinkage strain as in Eq. (18).

$$\epsilon_{sh}(t, t_c) = \epsilon_{shu} \beta(h) \beta(t - t_c) \tag{18}$$

The latter results from the multiplication of the ultimate shrinkage strain ϵ_{shu} and the correction coefficient Eq. (19) function of the ambient relative humidity h , and by the time-dependent function Eq. (20), where t is the present concrete age, t_c is the concrete age at the drying beginning and V/S is the volume to surface ratio in millimeters.

$$\beta(h) = (1 - 1.18h^4) \tag{19}$$

$$\beta(t - t_c) = \left[\frac{(t - t_c)}{0.12(V/S)^2 + (t - t_c)} \right]^{1/2} \tag{20}$$

The GL 2000 model does not consider the chemical admixtures information or the concrete mineral additives or information on the ambient curing process. Distinctly from the ACI 209R-92 model, the B3 model, and the EC2 shrinkage model, the GL 2000 model considers the volume to surface ratio V/S to account for the shape and size effect of the concrete element as a time function $\beta(t - t_c)$ to describe the shrinkage evolution.

Shrinkage model of fib model code 2010

The shrinkage model of the fib Model Code 2010 is strongly associated with the CEB MC90-99 model. The fib shrinkage model defines the notional drying shrinkage coefficient as in Eq. (21).

$$\epsilon_{cds0}(f_{cm}) = [(220 + 110\alpha_{ds1}) \exp(-\alpha_{ds2}f_{cm})] \times 10^{-6} \tag{21}$$

The latter is a function of several coefficients as well as the mean compressive strength of the concrete at 28 days f_{cm} , the coefficients α_{ds1} and α_{ds2} , both accounting for the cement type. The progress of the drying shrinkage deformation Eq. (22) is the result of multiplying the notional drying shrinkage coefficient $\epsilon_{cds0}(f_{cm})$ by the factor β_{RH} Eq. (23) in

order to consider the impact of ambient relative humidity RH (in %) and by the time-dependent function Eq. (24).

$$\epsilon_{cds}(t, t_s) = \epsilon_{cds0}(f_{cm}) \beta_{RH}(RH) \beta_{ds}(t - t_s) \tag{22}$$

$$\beta_{RH}(RH) = -1.55 \left[1 - \left(\frac{RH}{100} \right)^3 \right] \text{ for } 40 \leq RH < 99\% \tag{23}$$

$$\beta_{ds}(t - t_s) = \left(\frac{(t - t_s)}{0.035h^2 + (t - t_s)} \right)^{0.5} \tag{24}$$

The latter is a function of the concrete present age t , the concrete age at the drying beginning t_s and on the notional size $h = 2 \cdot A_c/U$ of the concrete element. Similar to the GL 2000 model, shape and size impact in the fib shrinkage model is just taken into account in the time-dependent function $\beta_{ds}(t - t_s)$ by the notional size h . As reported in [10], the time-dependent function Eq. (24) is unsure for concrete elements with $h \geq 600$ mm and can overrates the shrinkage deformations after 50 years of drying. Thus, the fib shrinkage model application is restricted by the notional size of the concrete element. In accordance with [11], additional investigative studies concerning the notional size coefficient is required. The fib model does not take note of either the period of moist curing or the curing temperature, which is intended for estimating shrinkage deformations of moist-cured concrete elements at normal temperatures for a period not exceeding 14 days.

Modeling

In the present case, the drying shrinkage evolution is described by a curvature that starts by exponential shape thence it advances towards an asymptotic limit, as shown in Fig. 1. In statistics, this form of shape matches with the curve of the density probability function $F(t, t_0)$ obtained with direct integration of the density probability function $f(t, t_0)$ in function of time (t), as seen in Fig. 2.

Figure 3 shows a reduction in the shrinkage for 14 and 28 days when the relative humidity tends to increase. By comparison, the shrinkage initially increases significantly for higher ages and then decreases

In this case of study, the probability density function $f(t, t_0)$ given in Eq. (25) is two parameters Weibull function [12]:

$$f(t, t_0) = \frac{c}{t - t_0} \times \left(\frac{t - t_0}{t - t_0} \right)^{c-1} \times \exp \left\{ - \left(\frac{t - t_0}{t - t_0} \right)^c \right\} \tag{25}$$

Such that $t - t_0 > 0$, where t_0 is the loading time (in days), $f(t, t_0)$ is a probability density function, and C represents the acceleration rate of the probability density function [13].

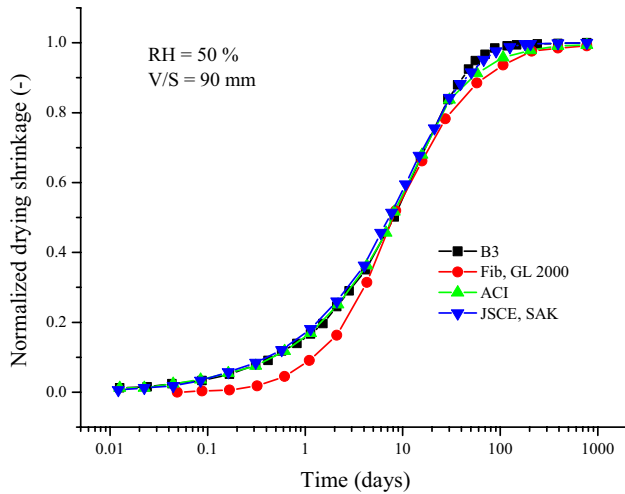


Fig. 1 Normalized drying shrinkage evolution [4]

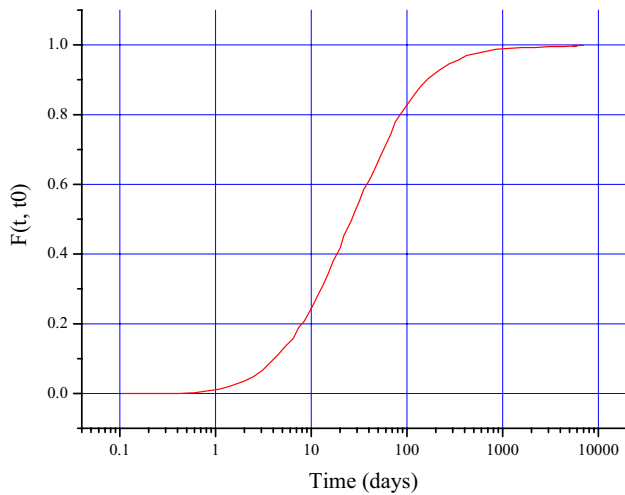


Fig. 2 Probability density function $F(t, t_0)$ [9]

$$b = (t - t_0)^{-C} \Rightarrow b = \frac{1}{(t - t_0)^C}$$

and $y = t - t_0$.

Hence, Eq. (25) becomes as follows:

$$f(t, t_0) = \frac{c}{(t - t_0)} \times \frac{(t - t_0)^{c-1}}{(t - t_0)^{c-1}} \times \exp \left\{ \frac{(t - t_0)^C}{(t - t_0)^C} \right\} \Rightarrow f(t, t_0) = c \times \frac{(t - t_0)^{c-1}}{(t - t_0)^C} \times \exp \left\{ \frac{(t - t_0)^C}{(t - t_0)^C} \right\} \quad (26)$$

Therefore;

$$f(t, t_0) = c \times b \times y^{c-1} \times \exp(-b \times y^C) \quad (27)$$

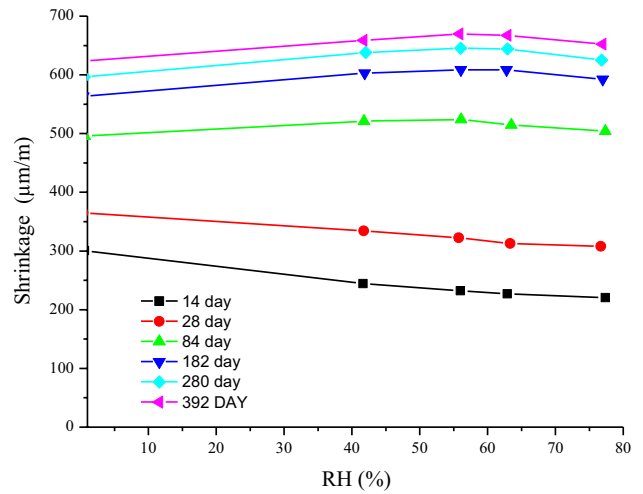


Fig. 3 Relative humidity RH effect on the shrinkage of concrete at different ages [3]

The probability density function is given by:

$$F(t, t_0) = \int f(t, t_0) dt \quad (28)$$

Proceed to the development of Eq. (28)

$$\text{Such as } F(t, t_0) = \int_{-\infty}^0 f(t, t_0) dt + \int_0^t f(t, t_0) dt \quad (29)$$

$$\int_{-\infty}^0 f(t, t_0) dt = 0 \quad (30)$$

Replace the function $f(t, t_0)$ by the equation in the integral as follows:

$$F(t, t_0) = \int_0^t (c \times b \times (t - t_0)^{c-1} \times \exp(-b \times (t - t_0)^C)) \cdot dt \quad (31)$$

Let:

$$v = b \times (t - t_0)^C \Rightarrow v' = c \times b \times (t - t_0)^{c-1} \quad (32)$$

by replacing v and v' in Eq. (29), we obtain $\int v' \times e^{-v} = -e^{-v}$.where

$$F(t, t_0) = -e^{-b(t-t_0)^C} \Big|_0^t = 1 - e^{-b(t-t_0)^C} \quad (33)$$

To consider the development of the density probability function $F(t, t_0)$ to reach an asymptotic limit, Eq. (9) is multiplied by a nonzero positive number “ a ” which yields to the final form:

$$F(t, t_0) = a \times (1 - e^{-b(t-t_0)^c}) \tag{34}$$

In this case study, the function $F(t, t_0)$ represents the degree of progress of drying shrinkage $\varphi(t, t_0)$ where:

$$\phi(t, t_0) = a \times (1 - e^{-b(t-t_0)^c}) \tag{35}$$

Estimation of the model parameters

To identify the model parameters, the results of tests given by Bazant [6] were used. These test series involve 35 cylindrical samples of diameter 160 mm and 36 cylindrical samples of diameter 83 mm. Also, three cylindrical samples of 300 mm diameter are also measured. The length of all cylinders is double their diameter.

The most appropriate and simplest method for estimating the parameters of linear models is the least-squares method [14]. This method consists of minimizing the differences between the regression line and the explained variable “y”. In other words, it reduces the sum of the squares also called the “sum of the squares of the residues” denoted “SCR”.

$$SCR = \sum_{i=1}^N \epsilon_i^2 \tag{36}$$

With, $\epsilon_i = y_i - \hat{y}_i$: error at the point t between the measured and calculated value.

The $\hat{\beta}$ estimation is the value of β which renders the expression (36) minimal

$$y_i = \hat{\beta}_0 + \hat{\beta}_1 x_{1i} + \hat{\beta}_2 x_{2i} + \dots + \hat{\beta}_k x_{ki} + \epsilon_i \tag{37}$$

The matrix form of this expression is:

$$y_N = X_{Nk} \cdot \hat{\beta}_k + \epsilon_N \tag{38}$$

The system (38) resolution allows the determination of the $\hat{\beta}$ estimator.

$$\hat{\beta} = (X' \cdot X)^{-1} X' \cdot Y \tag{39}$$

The degree of validity of a regression model is based on the following conditions [13]:

- The \bar{R}^2 must be as high as possible.
- Student’s and Fisher’s tests must provide acceptable results.
- The standard deviations of the coefficients must be the lowest for the estimated values of the coefficients.

From the set of observations on the model variables selected during this present study, several expressions by multiple regressions giving the parameters of the model have been proposed in Eq. (35); the expressions retained are given by the relations (40), (41), and (42).

$$a = \beta_1 + \beta_2 \cdot (RH)^2 + \beta_3 \left(\frac{V/S}{RH} \right) \tag{40}$$

$$b = \beta_4 + \beta_5 \cdot (V/S) + \frac{\beta_6}{RH} \tag{41}$$

$$c = \beta_7 + \beta_8 \cdot ((V/S)^2 \cdot (RH)) \tag{42}$$

With: V/S = volume to surface area ratio of concrete elements in (mm), and RH = relative humidity in (%).

The test’s parameters of model coefficients a , b and c are given in Tables 1, 2, and 3.

Improvement of the model

Adjusting the parameter «a»

The parameter «a» represents the limit value of drying shrinkage. This parameter is influenced by the relative humidity conditions RH and by the V/S ratio of the element [3]. The relative humidity is one of the most essential factors affecting the final shrinking of the concrete.

Figure 4 discusses the influence of the V/S ratio on the shrinkage measured for various concrete ages. The higher the V/S ratio, the lower the shrinkage.

A statistical analysis founded on experimental results given by [7] shows that the values of the parameter «a» are mostly between (300 and 600 $\mu\text{m}/\text{m}$) as illustrated in Fig. 5.

Table 1 «a» Parameter tests

Model coefficients	Standard deviation	Student’s test		Fisher’s test		Correlation coefficient		
		T_{Student}	$P(S)^*$	T_{Fisher}	$P(F)^{**}$	R^2	\bar{R}^2	
β_1	1.25004	0.0155	80.640	0.00	682.51	0.0000	0.9572	0.9558
β_2	-0.8423	0.0267	-30.828	0.00	682.51	0.0000	0.9572	0.9558
β_3	-0.0012	0.0001	-9.6071	0.00	682.51	0.0000	0.9572	0.9558

Table 2 «b» Parameter tests

	Model coefficients	Standard deviation	Student’s test		Fisher’s test		Correlation coefficient	
			$T_{Student}$	$P(S)^*$	T_{Fisher}	$P(F)^{**}$	R^2	\bar{R}^2
β_4	0.236297	0.0027	85.8150	0.00	1071.38	0.0000	0.9723	0.9714
β_5	-0.00400	8.7E-05	-45.890	0.00	1071.38	0.0000	0.9723	0.9714
β_6	0.002927	0.0004	6.0662	0.00	1071.38	0.0000	0.9723	0.9714

Table 3 «c» Parameter tests

Model coefficients	Standard deviation	Student’s test		Fisher’s test		Correlation coefficient		
		$T_{Student}$	$P(S)^*$	T_{Fisher}	$P(F)^{**}$	R^2	\bar{R}^2	
β_7	0.540896	0.0037	144.6832	0.0000	682.517	0.0000	0.7901	0.7202
β_8	3.13E-05	8.9E-06	3.5082	0.0127	682.517	0.0000	0.7901	0.7202

$P(S)^*$: probability of significance of each estimated coefficient
 $P(F)^{**}$: probability of significance associated with T_{Fisher} value

Adjusting the parameter «c»

The variation of the «c» parameter is a relative humidity RH and V/S ratio function as reported in Table 4. Note that the «c» parameter values vary little and are close to 0.5.

Adopting $c=0.5$, the equation yielding the progression of the drying shrinkage is reduced to an expression with two parameters:

$$\phi(t, t_0) = a \times (1 - e^{-b(t-t_0)^{0.5}}) \tag{43}$$

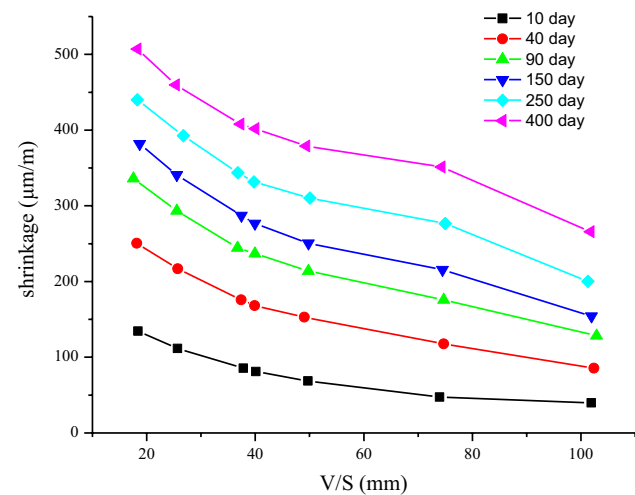


Fig. 4 V/S ratio effect on the shrinkage of concrete at different ages [3]

Validation of the model

To check the proposed model accuracy, we first compare the model predictions with normal concrete (NC), high-performance concrete (HPC), lightweight concrete (LWC), and self-compacting concrete (SCC) as well as with most common models by means of available databases.

Comparison of model predictions with normal concrete experimental values [6] given by Bazant

Figure 6a shows the contribution of the drying shrinkage for a constant volume to surface area ratio $V/S=152$ mm and variable environmental relative humidity RH (40%, 60%, and 80%), as well as constant environmental relative humidity of $RH=65\%$ and variable V/S ratio (76; 152; 304 and 610 mm) in Fig. 6b.

Curves in Fig. 6a show the influence of relative humidity RH for constant V/S ratio on predicted drying shrinkage.

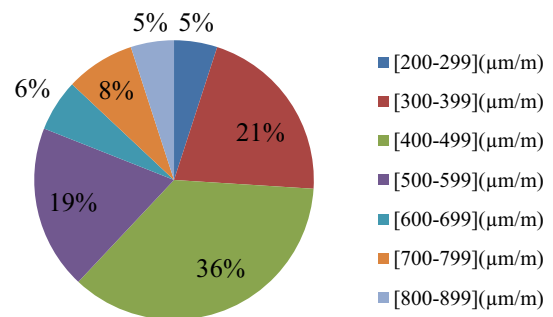


Fig. 5 Proposals of the values by intervals of the parameter «a» (µm/m)

Table 4 «c» Coefficient values estimated by the “SCR” method

V/S (mm)	RH (%)	c	V/S (mm)	RH (%)	c	V/S (mm)	RH (%)	c
76	20	0.591	102	20	0.536	152	20	0.599
76	50	0.443	102	50	0.508	152	50	0.576
76	75	0.511	102	75	0.525	152	75	0.653

This influence is less nuanced at younger ages to around 120 days, but it clearly appears at advanced ages. It is even observed on the curves of Fig. 6a that the amplitude of both drying shrinkage models increases inversely with the decrease in the relative humidity RH. The curves in Fig. 6b illustrate the influence of the V/S ratio. It is noted that the effect of this latter is more marked. It seems that the drying shrinkage decreases with increasing V/S ratio of specimens.

Confronting drying shrinkage model evolution of high-performance concrete (HPC) with experimental results of vahid [15]

Drying shrinkage leads to cracking of high-performance concrete (HPC), thereby reducing its strength and durability.

Regardless of the benefits of HPC in comparison with standard concrete, the mineral additives existence in HPC can enhance the risk of early age cracking that may reduce the lifetime of the concrete structures. Furthermore, for large surface area concrete buildings, drying shrinkage is critical and may decrease the durability and concrete strength due to cracks development [16].

As described above, the concrete drying shrinkage deformations were predicted by several developed models. Nevertheless, it is generally known that the mentioned

characteristics are rated as the most unpredictable concrete behavior. The comparisons between the model’s predicted values and drying shrinkage experimental results given by [15] are presented in Fig. 7.

The results of 03 mixes with different fiber-reinforced concretes as well as SF10GGBS30 (The Silica Fume SF and Ground Granulated Blast-Furnace Slag GGBS were added as cement replacements for the amounts of 10% and 30% of cement weight, respectively), 0.6HE (Hooked-End steel fibers with 0.6% fiber volume fraction), and 1.2DHE (Double Hooked-End steel fibers with 1.2% fiber volume fraction) have been confronted to different models predicted values. Figure 7 illustrates that all those models present a comparable curve with the measured experimental results.

As Fig. 7 illustrates, both ACI and Euro code 2 models considerably over-predict the drying shrinkage of all the three mixes chosen in this comparison. However, the developed model under predicts the early age shrinkage of concretes and over predicts it beyond 150 days of drying as well as the *fib* model presents the same trend beyond 100 days for the mix 1.2 DHE. Both *fib* and the developed model present a good concordance with experimental results for the mix 0.6HE and some divergence was observed in the final drying shrinkage rate for the mix SF10GGBS30.

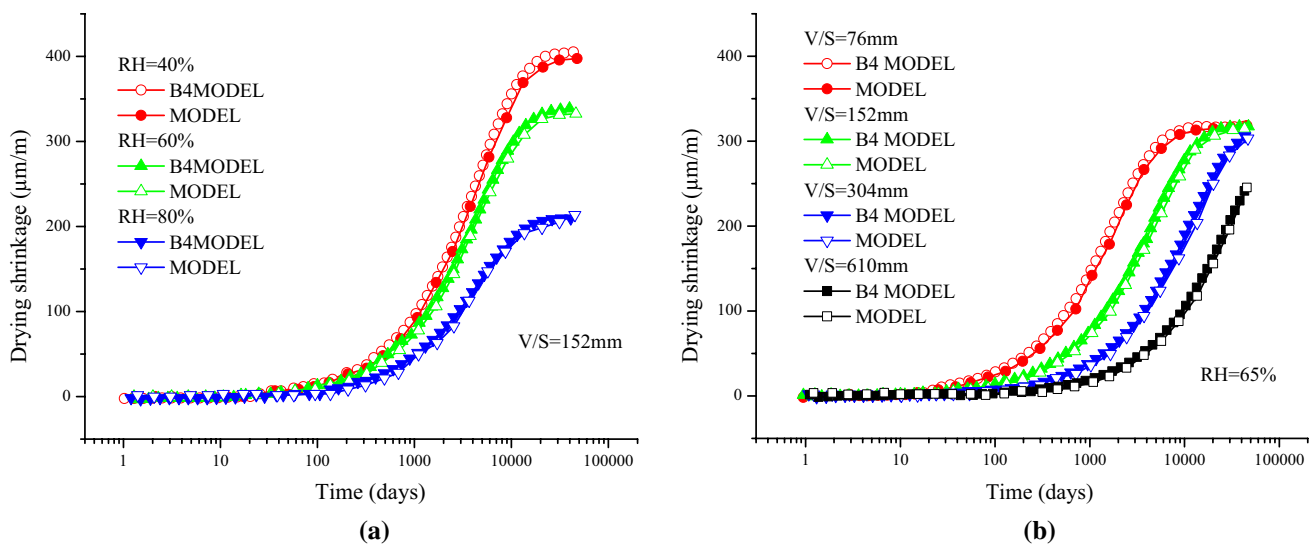


Fig. 6 Predictions of drying shrinkage curves as a function of varying V/S ratio and humidity confronted to B4 model given by Bazant [6]

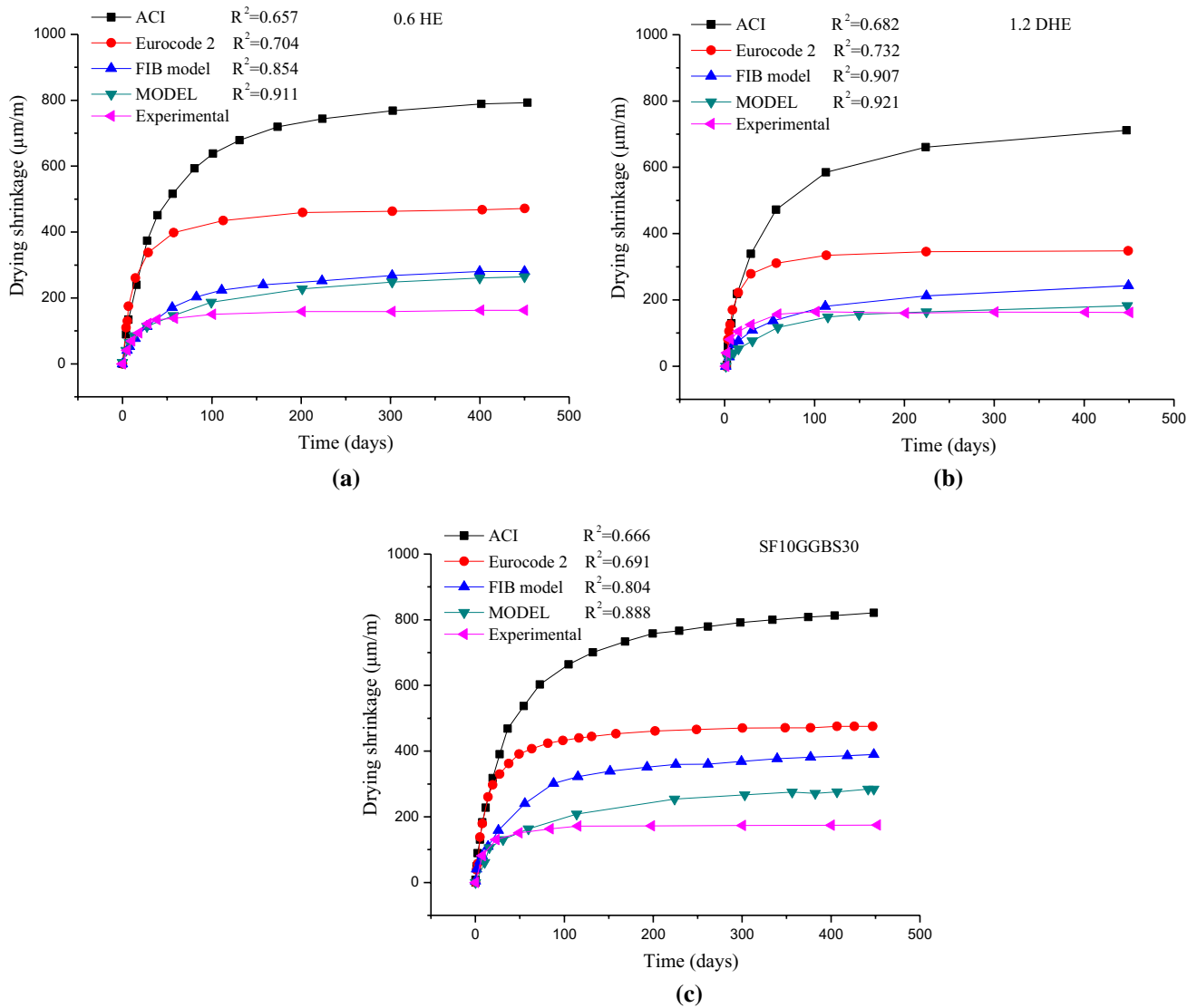


Fig. 7 Confrontation of models predictions and experimental results of drying shrinkage [15] for different mixes: **a** 0.6DHE, **b** 1.2DHE, **c** SF10GGBS30

It was, furthermore, noticed that the developed model provides the highest accuracy between the compared models when predicting concretes shrinkage with different fibers admixtures. The higher accuracy of this model can be interpreted by the fact that the quality of the shrinkage predictive model depends on the contribution of each parameter that conducts the phenomena as well relative humidity RH and volume to surface area ratio V/S . However, the impact of cement substitution with mineral admixtures and the fibers incorporation has not been considered by this model as well as by other models. Hence, the inaccurate predictions of the ACI and Euro code 2 models can be explicated by the lack of aforementioned parameters in its equations.

Confronting drying shrinkage model predictions with lightweight concrete (LWC) experimental results

Short-term comparison

In the global construction industry, the need for modern innovation in the production of lightweight concrete has increased. Research into alternative lightweight concrete systems for structural applications are therefore more often needed. Foamed concrete (FC), likewise called cellular concrete, acquires important focus from researchers all around the world. FC offers special qualities namely acoustic and thermal isolation, thermal attack and fire resistance, lowers building costs, and delivers low weight characteristics.

Figure 8 demonstrates the confrontation between the drying shrinkage deformations of structural fibred-foamed concrete SFFC containing different foam volumes of polypropylene PP (SFFC0.75PP and SFFC1.5PP) provided by [17] with models predictions.

Figure 8 illustrates the influence of PP fibers on the shrinkage predictions of FC specimens with different foam volumes along the drying time. The incorporation of a large volume of polypropylene PP fibers conspicuously reduced the drying shrinkage value.

The predicted drying shrinkage deformations of ACI, the developed model, and *fib* model for the SFFC0.75PP sample were between 1200 ($\mu\text{m}/\text{m}$) and 1400 ($\mu\text{m}/\text{m}$) after 175 days of drying with a correlation factor coefficients R^2 of 0.967, 0.981, and 0.978, respectively. After augmentation of the foam volume of polypropylene PP from 0.75 to 1.5%, the drying shrinkage prediction values of the SFFC0.75PP sample had prominently decreased to around 900 ($\mu\text{m}/\text{m}$). Nevertheless, the ACI, developed model and *fib* model are in a narrow range of structural fibred-foamed concrete drying shrinkage deformations for both mixes.

Long-term comparison

Figure 9a presents the comparison between the lightweight concrete drying shrinkage results provided by [18] and those predicted by ACI, *fib*, and the developed model.

The final average shrinkage of the ACI, *fib*, and the developed model was 753 $\mu\text{m}/\text{m}$, 818 $\mu\text{m}/\text{m}$, and 846 $\mu\text{m}/\text{m}$, respectively. The final shrinkage values of all prediction models were different. The shrinkage of *fib* model was higher than the two other models at early age to around 20 days when both achieved identical shrinkage rates. After

40 days, the curves show that the shrinkage rate of the ACI model tends to decrease, while the developed and *fib* model does not present similar progression throughout the drying period, which leads to larger gaps between shrinkage models predictions and LWC data.

The results from the thinner shrinkage samples with $V/S = 6.08$ mm were used for comparative analysis. The lower V/S enhances water diffusion, speeds up drying and hence drying shrinkage. The contrasts between the experimental results and the predictions of the shrinkage models are shown in Fig. 9b. It is mentioned that the efficiency of both models is reduced when predicting the shrinkage of the thinner samples ($V/S = 6.08$ mm) compared to the thicker samples ($V/S = 20$ mm). As shown in Fig. 9b, the best shrinkage predictions for the LWC experimental results are from the developed model with $R^2 = 0.961$, *fib* model with $R^2 = 0.867$, and then the ACI model with $R^2 = 0.853$, respectively.

In addition, the water motion from the lightweight aggregate (internal curing) may, furthermore, clarify the distinctions between the shrinking deformation development of the two sample sizes. Water loss was smaller in $V/S = 20$ mm samples than that in $V/S = 6.08$ mm samples. Thus, internal curing impact for $V/S = 20$ mm specimens was more pertinent, which leads to more efficient cement paste hydration; this leads to lower hydrated cement paste porosity and permeability and consequently lower water diffusion, as previously observed.

The efficiency reduction in the model in Fig. 9b can be linked to the drying and water diffusion within the concrete, which is identified not only by the V/S ratio but even by the internal water included in the lightweight aggregates and the diffusion coefficient.

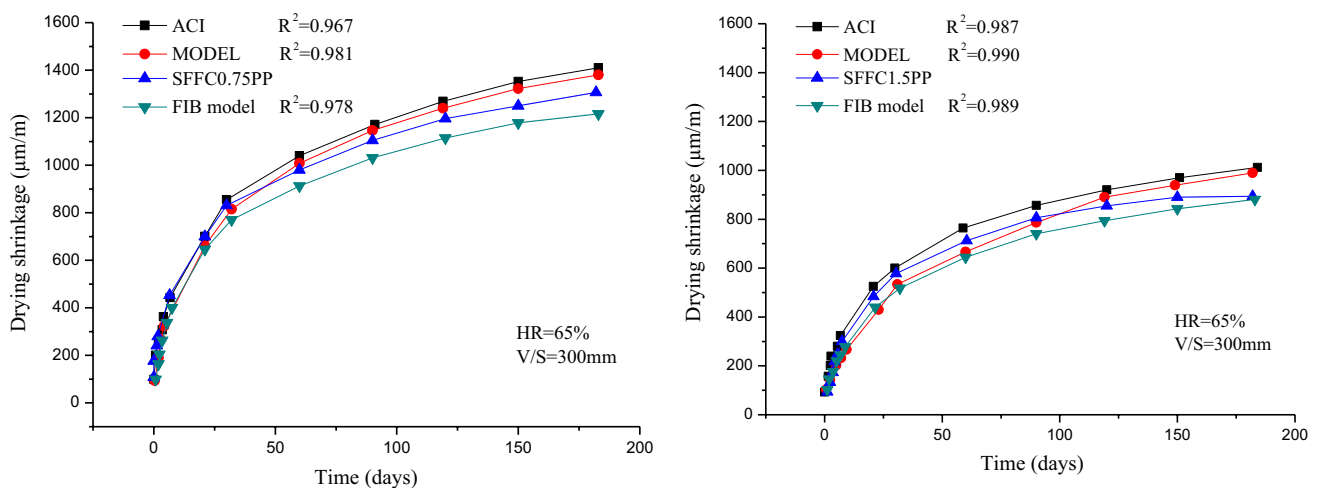


Fig. 8 Influence of foam volume of PP fibers on drying shrinkage deformation and models predictions [17]

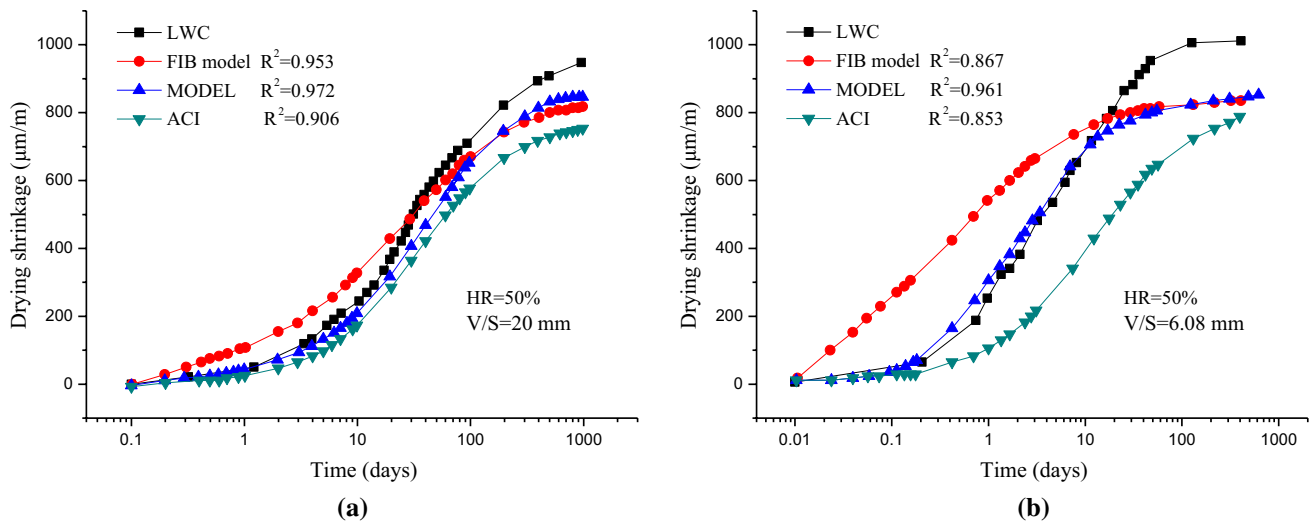


Fig. 9 Comparisons of the measured and models predicted drying shrinkage of **a** LWC for (HR = 50, V/S = 20 mm), and **b** LWC for (HR = 50, V/S = 6.08 mm) [18]

Confrontation of the model predictions with self-compacting concrete results

Drying shrinkage deformations can result into cracks in concrete constructions decreasing their performances as well as the service life and durability. As the concrete properties are an essential parameter for stress progress, self-compacting concrete (SCC) can present various behavior than conventional concrete.

Comparison with short-term drying shrinkage

In Fig. 10, the experimental results for four different self-compacting concrete mixes (self-compacting concretes with 5% and 15% silica fume were added as cement replacements (SCC5SF, SCC15SF) and self-compacting concretes with 20% and 60% fly ash were added as cement replacements (SCC20FA, SCC60FA)) given by [19] and the predicted values of different models are presented.

The comparison of the experimental and the predicted values result into the following conclusions:

- The ACI and the Eurocode2 prediction models are in a narrow range of experimental drying shrinkage deformations for all mixes, nevertheless, an over prediction of deformations is found beyond the first 15 days of drying for both models. It is also observed that the *fib* model presents a slight underprediction of the experimental deformations.
- All the prediction models have a good concordance with experimental results. However, the proposed model provides a better prediction of drying shrinkage for mixes SCC (5SF), SCC (15SF), SCC (20FA), and SCC (60FA)

with a coefficient of correlation factor R^2 of 0.972, 0.981, 0.971, and 0.987, respectively, compared to the experimental results.

- These modifications in the composition of the mixtures affect the behavior of the self-compacting concrete in its hardened state, including the drying shrinkage deformations. However, the prediction model’s efficiency has been influenced neither for ACI, Euro code 2, and *fib* model nor for the developed model.

Comparison with long-term drying shrinkage

Shrinkage in concrete presents the principal source of cracking in concrete structures. Volume contractions due to water loss from the concrete to the atmosphere are called drying shrinkage of concrete. This latter influences the structure’s load-carrying capability and deteriorates concrete strength. Crack’s evolution opens a path to the water as well as other chemical agents, which gradually disturbs the concrete cover and induces reinforcements corrosion. Thus a comparison of a long-term prediction is needed.

Figure 11 presents a confrontation for a long-term drying shrinkage sulfate resistance self-compacting concrete containing 20%, 60% of copper slag as cement replacements at various ages up to 450 days given by [20] and ACI, *fib* and developed models predicted deformations.

In addition to copper slag, the drying shrinkage of self-compacting concrete mixes was reduced, and the minimum predicted value of the drying shrinkage was obtained for the SCC20CS mix along the drying time. In general, drying shrinkage predictions for both models were similar at the earlier ages up to 28 days, whilst a slight difference was

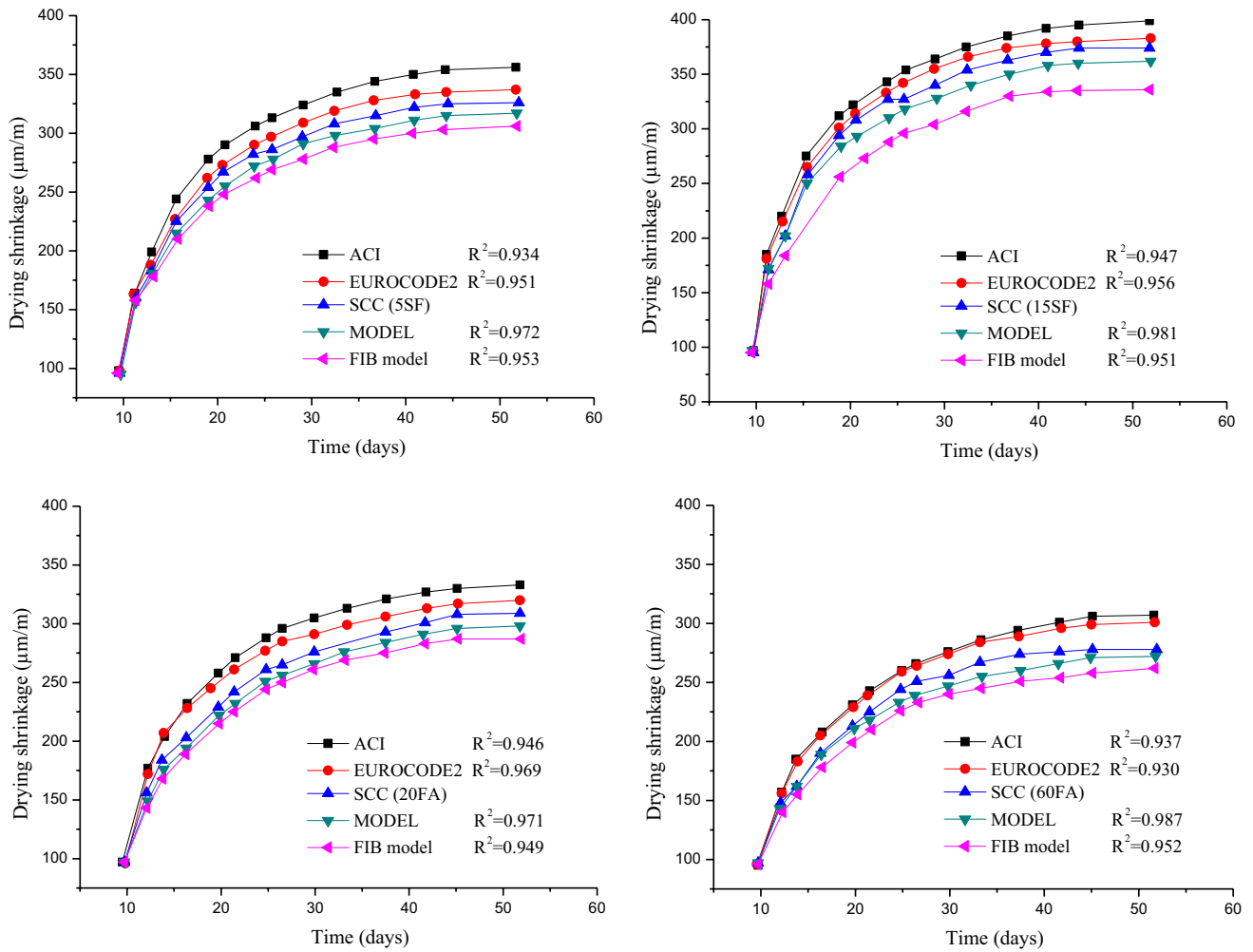


Fig. 10 The effect of mineral admixtures (SF and FA) on the drying shrinkage results [19] and models prediction for Self-compacting concretes

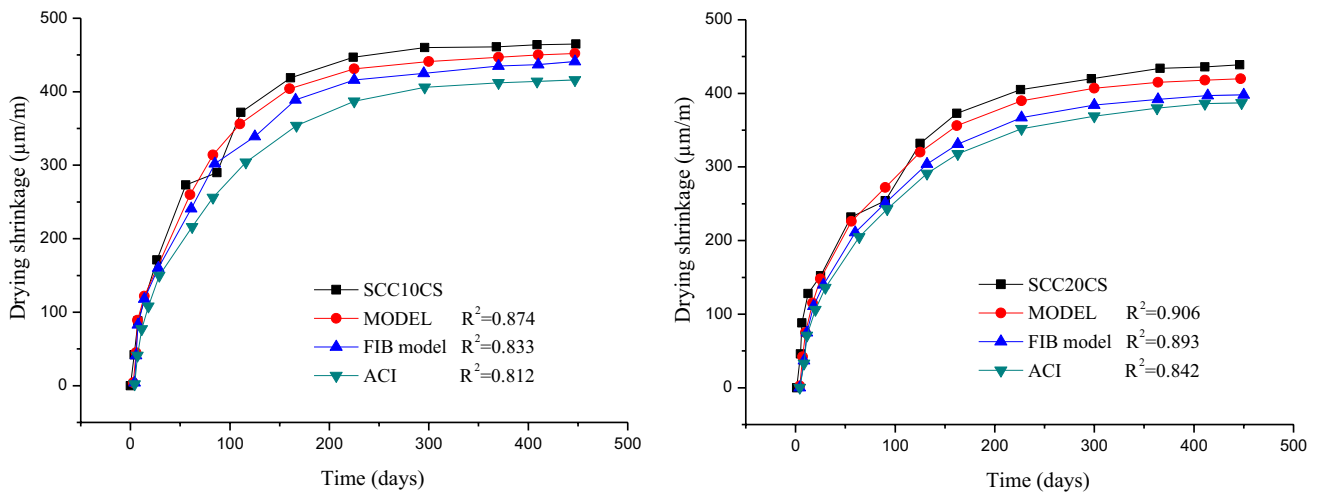


Fig. 11 Models predictions compared to drying shrinkage of SCC mixes containing 20%, 60% of copper slag [20]

noted beyond 28 days of drying time. The 28-day ACI, *fib*, and developed models predicted drying shrinkage values of self-compacting concrete prepared with 20% copper slag were 3.61%, 3.32%, and 2.37% lower than that of the SCC20CS mix. At 450 days, reductions in predicted shrinkage deformations for both models were 10.19%, 6.35%, and 5.87%, respectively, for the same mix composition. This could be related to the departure of physically absorbed water from C–S–H to the surroundings, resulting in drying shrinkage deformations.

Confrontation of developed model predictions with most common models and various databases

Confrontation with Al-Saleh [2]

Figure 12 provides a comparison of experimental measurements of drying shrinkage and theoretical drying shrinkage predictions applying the next five models: ACI [1], *fib* model [10], B3 [8], Sakata [21], and GL 2000 model [22]. Measures on samples were taken with $V/S = 125$ mm and various relative humidity $RH = 50\%$ and $RH = 5\%$.

Figure 12a illustrates that ACI and B3 models have the nearest predicted drying shrinkage for $RH = 50\%$, particularly when approaching ultimate drying shrinkage. At the start of the drying time, the ACI model under predicts experimental drying shrinkage whilst the B3 model slightly over predicts it. It can be noted from Fig. 12a that *fib* model at the drying beginnings is closed to the experimental drying shrinkage values. However, the model’s predicted deformations start to deviate as time goes towards ultimate shrinkage from experimental drying shrinkage deformations. Sakata expected drying shrinkage predictions are so close to the

experimental deformations along the first 40 days of drying time. Subsequently, the obtained values increased with a fast rate as the drying time goes towards the ultimate. Furthermore, GL 2000 model has the worst predictions from early age until the end of the drying period. The developed model predicts well the development of drying shrinkage compared to the results of experiments.

Figure 12b shows an augmentation of the final experimental drying shrinkage rate due to very low relative humidity $RH = 5\%$. The developed model and GL 2000 model describe well the evolution of experimental drying shrinkage. A rather large difference is observed at early and later ages for the rest of the models compared to experimental results. These imperfections are due to the presence of several parameters in those models.

Confrontation with Vinkler [23]

Three experimental specimens of $V/S = 200$ mm (mentioned as ST1), $V/S = 400$ mm (mentioned as ST2), and $V/S = 800$ mm (mentioned as ST3) and standard cylinders of $V/S = 75$ mm were used. Cylinders were separated into two sets of two samples and retained under diverse environmental conditions. The initial group (mentioned as V1–V2) was maintained in ambient conditions with $RH = 40\%$ when the second group (mentioned as V3–V4) was maintained in controlled conditions with $RH = 65\%$. Measured shrinkage data is compared with model predictions for all the different V/S and RH cited above as mentioned in Fig. 12.

The thicker specimen shrinks less as intended due to the slower drying process. The deformations in ST1, ST2, and ST3 are smaller compared with the shrinkage of cylinders.

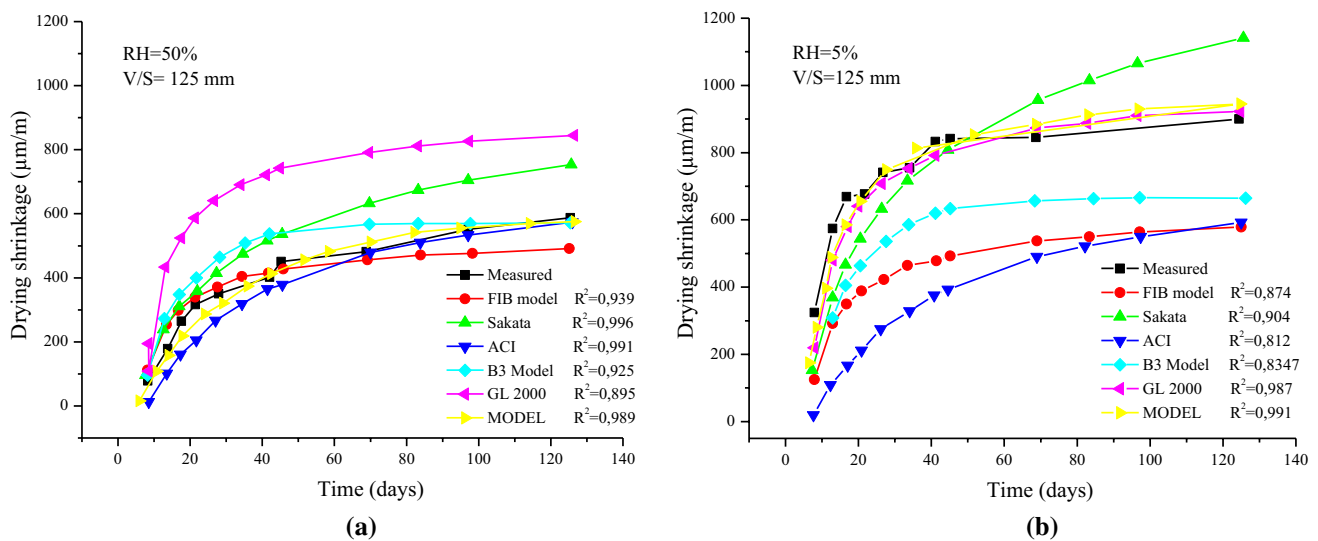


Fig. 12 Confronting model predictions and Al-Saleh [2] drying shrinkage experimental measures a $RH = 50\%$, b $RH = 5\%$

The far more interesting remarks from previous experimental data and model predictions are as follows:

- The size effect has been illustrated quite clearly in Fig. 13a. The higher is volume to surface area ratio, a slower shrinkage deformation was observed. The cause is obvious, thicker elements dry more slowly, because the moisture moves and travels over a longer distance in the element and so the drying shrinkage acts consistently. This result is in correlation with [24] and [23].
- Relative humidity variation affects directly the rate of drying shrinkage. The shrinkage rate increases with lower relative humidity conditions without influencing the prediction accuracy as shown in Fig. 13b.

Figure 14 presents a comparison of predicted drying shrinkage and several well-known shrinkage models as well as *fib* model [10], Euro code 2 [25], B4, B4S [5], and ACI [1].

From Fig. 14, we note that the models exhibit a fast increase in drying shrinkage at early age while the measured shrinkage development is slower. After a while, the rate of shrinkage prediction models is reduced. ACI and Euro code 2 models overestimate the evolution of drying shrinkage while B4 and B4S models underestimate it. The developed model and Fib’s model fit perfectly with experimental measurements at early ages and overestimate the evolution at later ages.

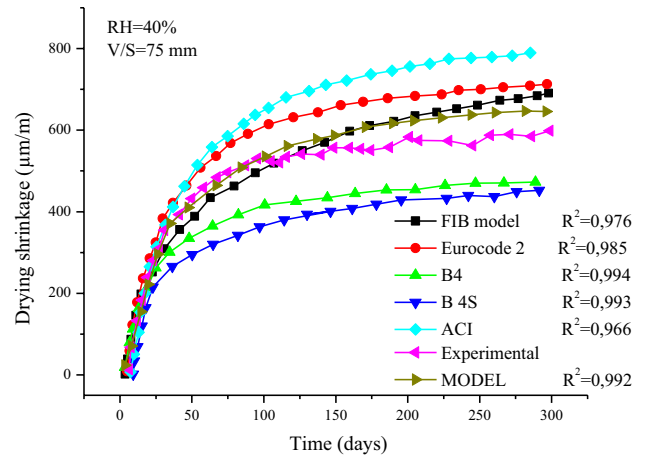


Fig. 14 Different models predictions compared with Vinkler experimental results [23]

The analysis of these curves clearly shows the concordance behavior that exists between the experimental results and those predicted by the developed model. However, a slight difference is observed only on a few curves at the early age, and sometimes at later ages compared to experimental results.

The developed model describes well the evolution of concrete drying shrinkage. Additionally, it presents better precision compared with the most common models.

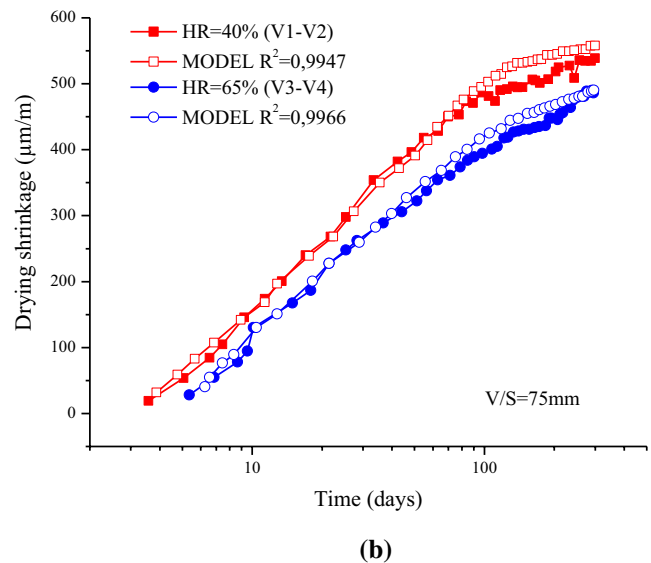
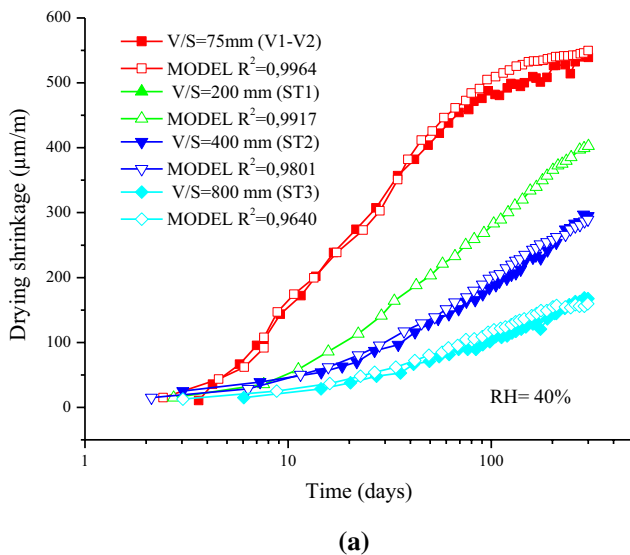


Fig. 13 Measured shrinkage data [23] compared with model predictions as a function of a V/S and b RH

Conclusion

The principal objective of this research was to develop a simplified predictive model with fewer affecting factors for drying shrinkage of structural concretes, namely for normal and high-performance concrete in order to predict the deformation rate during hardening. The main variables in the model are the volume to surface area ratio (V/S) and the relative humidity (RH). To reach this objective, we had based on a large number of experimental results obtained from various laboratories and some current and important codes of practice. This step leads us to summarize five essential points:

1. The developed model is well adapted to represent and describe the drying shrinkage evolution for normal concrete (NC), high-performance concrete (HPC), lightweight concrete (LWC), and self-compacting concrete (SCC), and it has been validated by comparison with various experimental results.
2. The model was developed and verified to predict the drying shrinkage deformations with different shrinkage affecting parameters. Relative humidity, size and shape of specimens, and mineral admixtures have a considerable effect on concrete drying shrinkage without influencing the prediction accuracy.
3. The final developed model is very simple and easy to use and it presents the advantage of containing only two parameters in comparison with the necessary parameters of other models.
4. The developed model can easily describe the drying shrinkage of concretes with more precision since the shrinkage strongly depends on desiccation.
5. It is a general model that applies particularly well to the range of conventional concretes and those with similar characteristics. Extreme cases require the introduction of corrective factors.

Funding Not applicable.

Code availability There is no code in this study.

Declarations

Conflict of interest The authors declare that there is no conflict of interest in presenting this manuscript.

Availability of data and material The data of this research is available.

References

1. McDonald DB, Brooks JJ, Burg RG et al (2014) Report on factors affecting shrinkage and creep of hardened concrete reported by ACI committee 209. *Am Concr Inst ACI 209(1)*:1–12
2. Al-Saleh SA (2014) Comparison of theoretical and experimental shrinkage in concrete. *Constr Build Mater* 72:326–332. <https://doi.org/10.1016/j.conbuildmat.2014.06.050>
3. Bal L, Buyle-Bodin F (2013) Artificial neural network for predicting drying shrinkage of concrete. *Constr Build Mater* 38:248–254. <https://doi.org/10.1016/j.conbuildmat.2012.08.043>
4. Bazant ZP, Murphy WP (1995) Creep and shrinkage prediction model for analysis and design of concrete structures—model B3. *Mater Constr* 28:357–365. <https://doi.org/10.1007/bf02486204>
5. Bažant ZP, Havlásek P, Jirásek M (2014) Microprestress-solidification theory: modeling of size effect on drying creep. *Comput Model Concr Struct Proc EURO-C 2014*:749–758
6. RILEM Technical Committee TC-242-MDC (Zdeněk PB chair) (2015) RILEM draft recommendation: TC-242-MDC multi-decade creep and shrinkage of concrete: material model and structural analysis*: Model B4 for creep, drying shrinkage and autogenous shrinkage of normal and high-strength concretes with multi-decade applicability. *Mater Struct Constr* 48:753–770. <https://doi.org/https://doi.org/10.1617/s11527-014-0485-2>
7. Bažant ZR, Li GH (2008) Unbiased statistical comparison of creep and shrinkage prediction models. *ACI Mater J* 105:610–621. <https://doi.org/10.14359/20203>
8. Bažant ZP (2001) Prediction of concrete creep and shrinkage: Past, present and future. *Nucl Eng Des* 203:27–38. [https://doi.org/10.1016/S0029-5493\(00\)00299-5](https://doi.org/10.1016/S0029-5493(00)00299-5)
9. Bazant ZP, Wittmann FH, Kim JK, Alou F (1987) Statistical extrapolation of shrinkage data—part I: regression. *ACI Mater J* 84:20–34. <https://doi.org/10.14359/1947>
10. International Federation for Structural Concrete (2012) fib Model Code 2010—Final Draft 1 and 2. *fib Bull* 65–66:350–374s
11. Muller HS, Kuttner CH, Kvitsel V (1999) Muller RFGC—creep and shrinkage models of normal and high-performance concrete—concept for a unified code-type approach. *Rev française génie Civ* 3:113–132
12. Scholz F (2002) Weibull Reliability Analysis. *Boeing* 5:1–76
13. Oger R, Saporta G (1991) Probabilités, Analyse des Données et Statistique. *Biometrics* 47:783. <https://doi.org/10.2307/2532171>
14. Concrete S (1990) Textbook on Behaviour. Des Performance Updat Knowl CEB/FIP Model Code 1
15. Afroughsabet V, Teng S (2020) Experiments on drying shrinkage and creep of high performance hybrid-fiber-reinforced concrete. *Cem Concr Compos* 106:103481. <https://doi.org/10.1016/j.cemconcomp.2019.103481>
16. Afroughsabet V, Biolzi L, Ozbakkaloglu T (2017) Influence of double hooked-end steel fibers and slag on mechanical and durability properties of high performance recycled aggregate

- concrete. *Compos Struct* 181:273–284. <https://doi.org/10.1016/j.compstruct.2017.08.086>
17. Amran YHM (2020) Influence of structural parameters on the properties of fibred-foamed concrete. *Innov Infrastruct Solut* 5:16. <https://doi.org/10.1007/s41062-020-0262-8>
 18. Labbé S, Lopez M (2020) Towards a more accurate shrinkage modeling of lightweight and infra-lightweight concrete. *Constr Build Mater* 246:118369. <https://doi.org/10.1016/j.conbuildmat.2020.118369>
 19. Güneysi E, Gesolu M, Özbay E (2010) Strength and drying shrinkage properties of self-compacting concretes incorporating multi-system blended mineral admixtures. *Constr Build Mater* 24:1878–1887. <https://doi.org/10.1016/j.conbuildmat.2010.04.015>
 20. Gupta N, Siddique R (2020) Sulfate resistance and drying shrinkage of self-compacting concrete incorporating copper slag. *J Mater Civ Eng* 32:04020389. [https://doi.org/10.1061/\(asce\)mt.1943-5533.0003501](https://doi.org/10.1061/(asce)mt.1943-5533.0003501)
 21. Sakata K, Shimomura T (2004) Recent progress in research on and code evaluation of concrete creep and shrinkage in Japan. *J Adv Concr Technol* 2:133–140. <https://doi.org/10.3151/jact.2.133>
 22. Gardner NJ, Lockman MJ (2001) Design provisions for drying shrinkage and creep of normal-strength concrete. *ACI Mater J* 98:159–167. <https://doi.org/10.14359/10199>
 23. Vinkler M, Vitek JL (2017) Drying shrinkage of concrete elements. *Struct Concr* 18:92–103. <https://doi.org/10.1002/suco.201500208>
 24. Gaylard PC, Ballim Y, Fatti LP (2013) A model for the drying shrinkage of South African concretes. *J South Afr Inst Civ Eng* 55:45–59
 25. Union E (2004) Eurocode 2: design of concrete structures—part 1–1: general rules and rules for buildings. *Br Stand Inst* 1:124–132